HHS Public Access

Author manuscript

Mol Microbiol. Author manuscript; available in PMC 2017 February 01.

Published in final edited form as:

Mol Microbiol. 2016 February ; 99(3): 557–570. doi:10.1111/mmi.13250.

Colony-morphology screening uncovers a role for the *Pseudomonas aeruginosa* nitrogen-related phosphotransferase system in biofilm formation

Matthew T. Cabeen, **Sara A. Leiman**, and **Richard Losick**

Department of Molecular and Cellular Biology, Harvard University, Cambridge MA 02138, USA

Summary

Pseudomonas aeruginosa is an opportunistic human pathogen whose survival is aided by forming communities known as biofilms, in which cells are encased in a self-produced matrix. We devised a mutant screen based on colony morphology to identify additional genes with previously unappreciated roles in biofilm formation. Our screen, which identified most known biofilm-related genes, also uncovered *PA14_16550* and *PA14_69700*, deletions of which abrogated and augmented biofilm formation, respectively. We also identified *ptsP*, which encodes enzyme I of the nitrogen-regulated phosphotransferase (PTS^{Ntr}) system, as being important for cyclic-di-GMP production and for biofilm formation. Further experiments showed that biofilm formation is hindered in the absence of phosphotransfer through the PTS^{Ntr}, but only in the presence of enzyme II (PtsN), the putative regulatory module of the PTS^{Ntr}. These results implicate unphosphorylated PtsN as a negative regulator of biofilm formation and establish one of the first known roles of the PTS^{Ntr} in *P. aeruginosa*.

Keywords

colony morphology; biofilms; mutagenesis; PTS^{Ntr}; GAF domain; cyclic-di-GMP

Introduction

The Gram-negative bacterium *Pseudomonas aeruginosa* is an important human opportunistic pathogen (Driscoll *et al*., 2007), especially in nosocomial pneumonia (Richards *et al*., 2000). Its success as a pathogen is in part driven by its ability to form biofilms. In a biofilm, a community of bacterial cells is held together and protected from the surrounding environment by a self-produced extracellular matrix generally comprising polysaccharides, DNA, and proteins (Hall-Stoodley *et al*., 2004). Biofilms enhance the resistance of bacterial cells to environmental insults such as antibiotic treatment (Drenkard & Ausubel, 2002, Nguyen *et al*., 2011), making chronic infections difficult to treat.

The extracellular polysaccharide (EPS) component of the biofilm matrix, termed Pel in strain PA14, is crucial for the ability of *P. aeruginosa* to effectively form a biofilm (Friedman & Kolter, 2004a). The synthesis of Pel is regulated both transcriptionally and post-

Correspondence: The Biological Laboratories, Harvard University, 16 Divinity Ave., Cambridge MA 02138. losick@fas.harvard.edu.

transcriptionally in response to various environmental signals by a complex regulatory network (Goodman *et al.*, 2004, Hickman *et al.*, 2005, Ventre *et al.*, 2006). One signal is an imbalanced intracellular redox state; cells lacking a terminal electron acceptor upregulate Pel production, as the resultant colony wrinkling allows cells better access to atmospheric oxygen (Dietrich *et al.*, 2013). As in many bacterial species (Boyd & O'Toole, 2012), the bacterial second messenger cyclic diguanylate (c-di-GMP) also has a central role in biofilm signaling in *P. aeruginosa* (Cotter & Stibitz, 2007). For example, the PelD protein directly binds c-di-GMP, and mutations that abolish c-di-GMP binding also prevent Pel production (Lee *et al.*, 2007b). Meanwhile, mutations that increase the intracellular c-di-GMP concentration, for instance by increasing the production or activity of diguanylate cyclases or decreasing the activity of phosphodiesterases, generally promote biofilm formation while suppressing non-biofilm behaviors such as cell motility (Kulasakara *et al.*, 2006). However, the existence of additional layers of biofilm regulation is evidenced by the absence of a strict correlation between intracellular c-di-GMP concentration and the degree of biofilm formation (Merritt *et al.*, 2010).

Many of the key regulators of *P. aeruginosa* biofilm formation, including the Pel proteins, multiple diguanylate cyclases and phosphodiesterases, upstream regulators, and cellular adhesion proteins, were discovered using a now-classic crystal violet-based screen for submerged biofilm formation in liquid medium (O'Toole & Kolter, 1998a, O'Toole & Kolter, 1998b). An alternative assay for biofilm formation relies on the visual inspection of bacterial colony morphology on solid biofilm-inducing media. Such an approach has proven useful for uncovering biofilm-related genes in bacterial species that do not form submerged biofilms in liquid culture, such as *Bacillus subtilis* (Branda *et al.*, 2006, Chu *et al.*, 2006, Kearns *et al.*, 2005, McLoonn *et al.*, 2011). In this approach, the appearance and degree of colony wrinkling is used as a proxy for biofilm formation, as the final morphology of a colony biofilm is an endpoint that reflects matrix production. Moreover, Congo red binding allows for quantification of the exopolysaccharide content of a homogenized colony. Different degrees of wrinkling by *P. aeruginosa* colonies have long been reported, and in fact the "rugose small-colony variant" phenotype that commonly appears in chronic human infections is associated with hyper-wrinkled colony morphology and elevated intracellular c-di-GMP concentration (Starkey *et al.*, 2009). Colony wrinkling and Congo red binding have been also been effectively used to monitor biofilm formation by *P. aeruginosa* (Friedman & Kolter, 2004b). However, colony wrinkling has not been used in a systematic screen to identify genes that affect *P. aeruginosa* biofilm formation.

Here, we report a colony morphology-based screen in *P. aeruginosa* for mutants altered in biofilm formation. The screen robustly identified known and unknown genes with different roles in biofilm formation, highlighting its effectiveness as well as its value as a tool for further discovery. We also describe three genes, identified using this screen, with distinct roles in biofilm formation that had not previously been appreciated.

Results and Discussion

A colony morphology-based screen for genes with roles in biofilm formation

As a means for discovering previously unrecognized genes that act within the biofilm regulatory network of *P. aeruginosa*, we employed a visual screen of colony morphology on agar plates (Fig 1A). We thus sought to find mutants with diminished or enhanced colony wrinkling. To facilitate the discovery of such mutant morphologies, we constructed a *amrZ* deletion mutant of strain PA14 for use as the parental strain in the screen, as it overproduces the Pel matrix exopolysaccharide and exhibits wrinkled colony morphology (Jones *et al.*, 2014) that we found easy to distinguish from flat or hyper-wrinkled morphologies. AmrZ, a transcriptional repressor, controls switching between an alginate-producing mucoid state and a Pel-producing biofilm state, such that the *amrZ* mutant is locked in the biofilm-producing state. An additional advantage of using an *amrZ* deletion strain was that it exhibits an approximately twofold elevated c-di-GMP level relative to the wild type (Jones et al., 2014). Elevated c-di-GMP is a phenotype that is associated both with stronger biofilm formation and with chronic infection (Starkey et al., 2009) and so our screen would also be expected to uncover genes that are required for such high c-di-GMP levels or augmented biofilm formation. In the case of the *amrZ* mutant, derepression of a gene that encodes a diguanylate cyclase enzyme, termed *adcA*, is thought to be largely responsible for the resulting rise in c-di-GMP levels and hence for enhanced biofilm formation (Jones et al., 2014).

Both previously characterized and unrecognized genes are identified by visual colony screening

We subjected the parental PA14 *amrZ* mutant strain to mutagenesis with a *Mariner*-based transposon (Kulasakara et al., 2006) and arrayed the resulting mutants on agar plates for visual inspection (Fig. 1A). We then verified the enhanced or diminished colony wrinkling phenotypes of the selected candidates and performed sequencing to identify the transposon insertion sites. We screened approximately 5,000 mutants and identified 119 candidates (Supplementary Table S1), representing a hit rate of approximately 2.4%. We found that the screen yielded genes spanning many of the known biofilm-related pathways (Fig. 1B; Supplementary Table S1). The number of independent hits per gene varied widely, ranging from genes that were only recovered once or twice to more-frequently recovered genes such as *pelA* (5 insertions) and *pilY1* (12 insertions, the most for any identified gene). Among many others, we identified *bifA*, which encodes a c-di-GMP-degrading phosphodiesterase (Kuchma *et al.*, 2007); *pilR*, *pilS*, *pilY1*, *fimV*, and *cupA5*, which encode surface-attachment proteins or their regulators (Alm *et al.*, 1996, Hobbs *et al.*, 1993, Ishimoto & Lory, 1992, Semmler *et al.*, 2000, Vallet *et al.*, 2001, Wehbi *et al.*, 2011); *hpd*, *phzA*, and *pqsL*, which encode or regulate quorum-sensing proteins and virulence factors (Ahuja *et al.*, 2008, Lepine *et al.*, 2004, Yoon *et al.*, 2007); *bswR*, which is involved in small RNA regulation (Wang *et al.*, 2014); *argC* and *argG*, which are involved in arginine metabolism (Haas *et al.*, 1977), and *pelA*, *pelC*, and *gacS*, which are involved in regulating or producing the exopolysaccharide matrix (Friedman & Kolter, 2004a, Parkins *et al.*, 2001). Some genes with known roles in biofilm formation, such as the diguanylate cyclase-encoding genes *sadC* (Merritt *et al.*, 2007) and *roeA* (Merritt et al., 2010) and the regulatory protein-encoding gene *wspF* (Hickman et al., 2005), were not detected by the screen. While genes whose main

roles are in surface attachment might be missed by a colony morphology-based screen, we primarily attribute such omissions to the screen not yet being close to saturation. Indeed, in a pilot screen using a similar parental background, we uncovered *roeA*. In sum, these findings demonstrate the ability of a colony morphology-based *P. aeruginosa* screen to uncover biofilm-related genes in an accurate, efficient, and unbiased manner.

In addition to the known genes uncovered by our screen, we also identified genes with no previously known roles in biofilm formation (Fig. 1C). These candidate biofilm genes included *PA14_16550* (orthologous to *PA3699*; hereafter *16550*), which encodes a TetR-type DNA repressor; *PA14_69700* (orthologous to *PA5279*; hereafter *69700*), which encodes an uncharacterized GAF-domain protein; and *ptsP*, which encodes enzyme I of the nitrogen-regulated phosphotransferase (PTS^{Ntr}) system. Insertions in these genes were recovered once, twice, and twice, respectively. Transposon disruption of *16550* and *ptsP* strongly diminished colony wrinkling, whereas the insertion in *69700* enhanced wrinkled biofilm morphology (Fig. 1C).

Deletion mutations of candidate genes perturb biofilm formation

To confirm that the altered colony morphologies of the mutants with insertions in *16550*, *69700*, and *ptsP* were a consequence of the inactivation of the respective genes, we constructed markerless, in-frame deletions of each gene in the parental *amrZ* mutant strain. Qualitative visual inspection of colony morphology confirmed that deletions of *16550* and of *ptsP* led to biofilm attenuation and that deletion of *69700* resulted in biofilm augmentation (Fig. 2A). The respective effects of the *16550* and *ptsP* deletions were each reversed by complementation of the deleted gene at the *attB* locus. The *69700* gene is located in the middle of an operon, and efforts to complement the deletion mutation have so far been unsuccessful. However, the original insertion mutant and the deletion mutant exhibit indistinguishable phenotypes, increasing our confidence that *69700* is indeed the relevant locus.

The qualitative colony morphologies were supported by quantitative biofilm measurements using Congo red binding (Fig. 2B). As expected, *amrZ* mutant colonies bound significantly more Congo red than the wild type (Fig. 2B, left graph). Our visual observations in the *amrZ* mutant background were confirmed by the Congo red data, as significant variations from the parental strain were apparent in the deletion mutants (Fig. 2B, right graph).

Biofilm formation is impaired by mutations of *16550* and ptsP and enhanced by *69700* mutation in otherwise wild-type cells

A key question was whether the deletion mutations of the genes we identified in our screen would exert a biofilm phenotype independently of the *amrZ* mutation. The deletion in *69700*, which increased biofilm formation in an *amrZ* mutant, did likewise in wild-type cells, visibly enhancing colony wrinkling (Fig. 2A) and increasing Congo red binding (Fig. 2B, center graph). Because wild-type PA14 colonies are relatively flat, it was difficult to visually distinguish the *16550* and *ptsP* mutations from the wild type by visual inspection (Fig. 2A). However, the *16550* mutant colonies bound slightly but detectably less Congo red than did the wild type (Fig. 2B, center graph). The *ptsP* mutant exhibited no significant

difference from the wild type in Congo red binding (Fig. 2B, center graph), but it did show a clear defect in biofilm mass as judged by crystal violet staining (Fig. 2C).

Mutations in 16550 and ptsP lower c-di-GMP levels

Because c-di-GMP is an important second messenger in biofilm formation, we next examined the effects of our candidate genes on cellular levels of the dinucleotide. We first asked whether a deletion in *16550*, which reduced colony wrinkling, correspondingly lowered c-di-GMP levels in the cells of a biofilm colony. For comparison, and as expected, the *amrZ* mutation elevated c-di-GMP levels roughly twofold (Fig. 3A). Interestingly, the *16550* deletion on its own caused a modest but significant increase in c-di-GMP (Fig. 3B). However, the *16550* mutation in combination with the *amrZ* mutation caused a significant decrease in c-di-GMP, lowering it to approximately wild-type levels (Fig. 3B). One possible interpretation of this result is that the 16550 protein, which encodes a TetR-type repressor, has multiple targets within the biofilm signaling network. For example, 16550 might be important for the transcription both of a *pel* gene and of a diguanylate cyclase-encoding gene that is upregulated in an *amrZ* mutant. In this case, deletion of *16550* would invariably lower matrix production by virtue of its *pel* regulation. However, it would only lower cyclic-di-GMP levels in the *amrZ* mutant.

Next, we examined the effect of the *ptsP* deletion. It caused a pronounced decrease in c-di-GMP levels both in a wild-type background and in a double mutant with the *amrZ* mutation. (Fig. 3C). Hence, the *ptsP* gene product appeared to have an important role in cellular c-di-GMP production under both wild-type and elevated-biofilm conditions.

The effects of 16550 and ptsP mutations are not mediated by AdcA

Because the *amrZ* mutation is known to cause derepression of *adcA*, which encodes a diguanylate cyclase (Jones et al., 2014), we hypothesized that the *16550* and *ptsP* deletions might be inhibiting *adcA* expression. As a first test, we constructed an *adcA* deletion to confirm its role in elevated biofilm formation. Surprisingly, when we examined the colony phenotype of an *amrZ adcA* double mutant strain, we observed no discernible change in colony morphology (Fig. S1A), suggesting that, in strain PA14 under our experimental conditions, AdcA plays only a minor role in the elevated-biofilm phenotype of the *amrZ* mutant. When we then analyzed the expression of *adcA*, it was indeed elevated in an *amrZ* mutant, but this derepression was not reversed by the 16550 mutation, and the *ptsP* mutation even caused a further elevation in expression (Fig. S1B). Collectively, these results appear to eliminate the hypothesis that the *16550* and *ptsP* mutations exert their effects by lowering the levels of the AdcA diguanylate cyclase. They also indicate that, in PA14, the inactivation of AmrZ provokes c-di-GMP synthesis by other pathway(s) in addition to *adcA* derepression.

Deletions of 16550 and ptsP inhibit hyper-biofilm formation by bifA and wspF mutants

We next asked whether *16550* and *ptsP* mutations would impair the hyper-biofilm phenotypes of other mutants (in addition to *amrZ*) that exhibit elevated c-di-GMP levels. We therefore introduced *16550* and *ptsP* mutations into mutants lacking BifA, a phosphodiesterase that degrades cellular c-di-GMP (Kuchma et al., 2007), and WspF, a

regulatory protein that inhibits the synthesis of the diguanylate cyclase WspR (Hickman et al., 2005). Both the *16550* and *ptsP* mutations substantially decreased colony wrinkling in the *bifA* and *wspF* mutants, with the *16550* mutant having a slightly stronger effect (Fig. 4A). Accordingly, Congo red binding assays showed substantial decreases from the *bifA* (Fig. 4B) and *wspF* (Fig. 4C) mutant strains. In addition, mutations of our newly identified biofilm genes significantly decreased cellular c-di-GMP concentrations in the *bifA* mutant background (Fig. 4D). We conclude that *16550* and *ptsP* mutations exert their negative effects on the hyper-biofilm phenotype of the *bifA* mutant by reversing the elevated levels of c-di-GMP. Interestingly, in the case of the *wspF* mutant, only the *ptsP* mutation significantly lowered the elevated levels of c-di-GMP (Fig. 4E). This result suggests that the *16550* mutation may have a distinct effect in the *wspF* mutant background that is not related to c-di-GMP production or clearance.

The role of PtsP in biofilm formation is independent of its GAF domain

We next turned our attention to PtsP, which is best-characterized among our three novel biofilm regulators and also the one with the most robust phentypes. PtsP is Enzyme I of the PTS^{Ntr} phosphorelay (EI^{Ntr}), which transfers phosphate groups from phosphoenolpyruvate (PEP), via Npr (encoded by *ptsO*), to Enzyme II (EII^{Ntr}, encoded by *ptsN*) (Fig. 5A) (Powell *et al.*, 1995, Rabus *et al.*, 1999, Zimmer *et al.*, 2008). The PTS^{Ntr} system (reviewed in (Pfluger-Grau & Gorke, 2010)) is paralogous to the canonical sugar PTS pathway that phosphorylates imported sugars to ensure their retention within the cell. However, unlike the EIIs of the canonical pathway, which transfer phosphate groups to sugars, EII^{Npr} has no known phosphorylation substrates; indeed, it lacks a second outward-facing His residue that is present in the sugar EII (van Montfort & Dijkstra, 1998). Instead, the PTS^{Ntr} is thought to exert its effects through protein-protein interactions. For example, in *Escherichia coli*, EII^{Ntr} interacts with TrkA and KdpD to regulate intracellular K^+ concentration (Lee *et al.*, 2007a, Lüttmann *et al.*, 2009). Additionally, unphosphorylated Npr (PtsO) interacts with LpxD in *E. coli* to decrease lipid A synthesis (Kim *et al.*, 2011). The phosphorylation state of the *E. coli* PTS^{Ntr} system appears to depend on the cellular glutamine/α-ketoglutarate ratio; a high ratio indicates nitrogen sufficiency and inhibits phosphotransfer, whereas nitrogen starvation stimulates the PTS^{Ntr} (Lee *et al.*, 2013). The responsiveness of the PTS^{Ntr} to glutamine and α-ketoglutarate appears to require the GAF domain of PtsP, as its deletion in *E. coli* preserved phosphotransfer but abolished small-molecule regulation (Lee et al., 2013).

We therefore asked whether the GAF domain of PtsP was required for its role in biofilm formation, reasoning that it might be involved in sensing in c-di-GMP. GAF domains are well-known for allosterically binding cyclic mononucleotides to regulate enzyme activity. Thus, it was possible that PtsP might be activated by c-di-GMP under biofilm-forming conditions to further stimulate c-di-GMP synthesis and biofilm formation. To test this possibility, we replaced the native chromosomal copy of *ptsP* with a version containing a markerless, in-frame deletion of the GAF domain-encoding sequence. We used the *amrZ* mutant background to facilitate the detection of any phenotypic differences. In contrast to the pronounced defect in biofilm formation caused by removal of the entire gene, the wrinkled colony morphology of the GAF domain mutant was neither altered (Fig. 5B) nor quantitatively different (Fig. 5C) from the *amrZ* mutant parental strain. Moreover, cellular c-

di-GMP was unchanged by the GAF deletion (Fig. 5D). This result indicates that the GAF domain is dispensable for the role of PtsP in biofilm formation.

PtsN is required for biofilm inhibition in the absence of upstream phosphotransfer

As PtsP is the most upstream enzyme in the PTS^{Ntr} phosphorelay (Fig. 5A), we examined (again using the *amrZ* mutant background to facilitate the detection of phenotypes) whether the effect of a *ptsP* deletion involved one or more of the remaining members of the PTS^{Ntr} system. We considered two possibilities. The first was that the role of PtsP in biofilm formation is independent of the PTS^{Ntr} system, whereas the second was that the phenotype of a *ptsP* deletion is caused by disrupted phosphate flow through the PTS^{Ntr} system. To distinguish these possibilities, we deleted *ptsO*, which encodes the Npr enzyme downstream of PtsP (Fig. 5A). In the first case, *ptsO* deletion would be expected to have little or no effect on biofilm formation. However, in the second case, *ptsO* deletion would also block phosphate flow through the PTS^{Ntr} and thus phenocopy the *ptsP* deletion. In fact, the phenotype of a *ptsO* null mutant resembled that of the *ptsP* mutant, exhibiting severely inhibited colony wrinkling and significantly less Congo red binding than the *amrZ* deletion alone (Fig. 6A–B). This finding suggested that strong biofilm formation requires phosphate flow through the PTS^{Ntr} system. It also confirmed that, as in *E. coli* (Lee et al., 2013), the GAF domain deletion of PtsP did not interfere with its phosphotransfer function, as removal of the PtsP GAF domain (in contrast to removing PtsO) had no effect on colony morphology as we have seen (Fig. 5B).

The phenotypic similarity of the *ptsP* and *ptsO* mutants prompted us to focus on PtsN, the EII^{Ntr} that is the final recipient of phosphates in the PTS^{Ntr} (Fig. 5A). Our results again raised two possibilities. First, phosphorylated PtsN might have a stimulatory effect on c-di-GMP levels and hence biofilm formation. In this case, deleting *ptsN* would phenocopy a *ptsP* or *ptsO* deletion, as it would eliminate PtsN function. Alternatively, unphosphorylated PtsN might have an inhibitory effect on biofilm formation. In this case, we would expect that deleting *ptsN* would have little or no effect on biofilm formation but that it would bypass the phenotype of a *ptsP* deletion by eliminating the effect of unphosphorylated PtsN. When we constructed an *amrZ ptsN* double mutant, we found that it exhibited wrinkled colony morphology and Congo red binding that did not significantly differ from those of the *amrZ* mutant strain (Fig. 6A–B), suggesting that PtsN is not required to stimulate biofilm development. Moreover, adding the *ptsN* deletion to an *amrZ ptsP* double mutant reversed the biofilm-inhibition phenotype of the *ptsP* mutation (Fig. 6A–B), arguing that the biofilm inhibition displayed by the *ptsP* and *ptsO* mutant strains is mediated by unphosphorylated PtsN. When we examined cellular c-di-GMP levels in these same strains, we observed that the *ptsN* deletion alone had no effect on c-di-GMP but that it rescued the lowered c-di-GMP levels of the *ptsP* deletion (Fig. 6C). Therefore, the PTS^{Ntr} system as a whole has an important role in biofilm formation. Phosphate flow through the PTS^{Ntr} ensures that PtsN remains phosphorylated, thus permitting elevation of c-di-GMP levels and strong biofilm formation. However, if the phosphorelay is blocked, unphosphorylated PtsN acts as an inhibitor of biofilm formation through a currently unknown mechanism.

69700 deletion enhances biofilm formation but does not increase c-di-GMP levels

Our screen also uncovered *69700*, deletion of which yielded an elevated-biofilm phenotype (Fig. 2). We thus suspected that it might increase c-di-GMP levels. However, the *69700* deletion only slightly increased c-di-GMP levels, not reaching statistical significance in either the wild-type or *amrZ* mutant backgrounds (Fig. 7A). When we constructed double deletions of *69700* with *wspF* or *bifA*, we also observed further enhancement in colony wrinkling in both backgrounds (Fig. 7B). Congo red binding confirmed that the *69700* mutation significantly increased biofilm formation in these backgrounds (Fig. 7C). However, when we analyzed the c-di-GMP levels of these double mutants, they again showed only a slight increase (Fig. 7D). Collectively, these results suggest that the substantial enhancement of colony morphology in a *69700* mutant is not primarily mediated through c-di-GMP signaling. Therefore, in contrast to 16550 and PtsP, the normal function of the 69700 protein appears to be as a negative, c-di-GMP-independent regulator of biofilm formation, as its deletion in all tested backgrounds enhanced biofilm formation, even under conditions in which biofilm signaling was already substantially upregulated.

Perspectives and outlook

The present work demonstrates the value of colony morphology for the discovery of previously unrecognized genes involved in biofilm formation, as we identified three such genes. Of special interest was the *ptsP* gene, whose robust phenotype allowed us to show that the *P. aeruginosa* PTS^{Ntr} has a role in c-di-GMP production and biofilm formation—the first established function of the PTS^{Ntr} in this species. We also identified *16550* as being needed for efficient biofilm formation. The *16550* gene encodes a TetR-type repressor whose PAO1 homolog (PA3699) binds to the promoter region of the gene encoding the LasR quorum-sensing regulator (Longo *et al.*, 2013). However, whereas PA3699 repressed *lasR* transcription when overexpressed from a plasmid, its inactivation had no detectable effect on *lasR* (Longo et al., 2013), leading us to conclude that the biofilm-related role of the 16550 protein is distinct from a role in *lasR* repression. The third newly identified gene, *69700* (*PA5279* in PAO1), is notable because its product inhibits biofilm formation and because it contains a crystallographically validated GAF domain of unknown function (PDB 3E98). GAF domains are generally considered small ligand-binding domains, but the functions of most GAF domains are not well-understood (Heikaus *et al.*, 2009). Our initial results indicate that 69700 does not act via c-di-GMP signaling, implying that it impedes biofilm formation via some other yet-to-be elucidated pathway. Not only have the discovery of *ptsP*, *16550*, and *69700* raised important unanswered questions about the circuitry governing biofilm formation, but our screen has not yet reached saturation and we anticipate that additional genes involved in biofilm formation remain to be discovered.

Experimental Procedures

Strains and growth conditions

Escherichia coli SM10 and *Pseudomonas aeruginosa* PA14 were grown in Luria-Bertani (LB) broth (10 g/L tryptone, 5 g/L yeast extract, 5 g/L NaCl) or on LB agar plates fortified with 1.5% Bacto agar at 37°C. When appropriate, 25 μg/ml irgasan (to specifically select for *P. aeruginosa*) plus 75 μg/ml tetracycline, 25 μg/ml irgasan plus 75 μg/ml gentamicin, 25

μg/ml tetracycline, or 20 μg/ml gentamicin was added to liquid or solid medium. The strains used in this work are listed in Table 1 and Supplementary Table S2. Markerless deletions were generated using the pEXG2 vector with counterselection on LB plates containing 6% sucrose and were screened by colony PCR for the presence of deletions. Complementation and reporter strains were constructed by integration of the mini-CTX-1 vector at the neutral chromosomal *attB* locus. Plasmids, primer sequences, and modes of strain construction are listed in the Supplementary Information.

P. aeruginosa biofilm studies were conducted using liquid or solid (1% agar) M6301 or M6301R medium. M6301 medium is composed of 100 μM KH_2PO_4, 15.14 mM $(NH_4)_2SO_4$, and 0.36 μM $FeSO_4{\cdot}H_2O$ (pH-balanced to 7.0 using 10 M KOH) (Cabeen, 2014); after autoclaving and before use, 0.5% glycerol, 1 mM $MgSO_4$, and 0.2% casamino acids (BD Bacto, USA) were added.

Transposon mutagenesis and biofilm colony morphology screen

P. aeruginosa PA14 Δ*amrZ* (MTC590) and *E. coli* SM10 pBT24 (MTC33) were grown as separate liquid cultures in 3 ml of LB for 6–8 h at 37°C in a tube roller. An aliquot of MTC33 (50 μl) was spot-dried on LB agar plates, and 100 μl of MTC590 was spot-dried atop the dried MTC33. The plates were incubated overnight at 37°C. The following day, the cells were harvested and resuspended in 500 μl sterile phosphate-buffered saline (PBS; 20 mM potassium phosphate, 150 mM NaCl) and plated for single colonies on LB agar containing irgasan and gentamicin. Individual single colonies were picked and used to inoculate LB (150 μl/well) in 96-well plates (Costar, Fisher Scientific, USA). The 96-well plates were incubated overnight at 37°C. Each plate contained 2 cultures each of PA14 and MTC590 as reference samples.

Cells from the 96-well plate cultures were deposited with a 6-by-8 48-pin array onto M6301 agar plates and grown at 25°C. At days 4 and 6, colonies exhibiting a biofilm morphology that differed from that of MTC590 were imaged and streaked for single colonies on LB agar with gentamicin. These colonies were then grown in 3 ml LB culture with gentamicin, and aliquots were archived in frozen glycerol (25% final concentration) stocks. A 2-μl sample of each culture was then spotted on M6301 agar to verify the initially observed colony morphologies. Colonies that exhibited reproducible colony morphologies were subjected to sequencing with the primer BT20TnMSeq following two rounds of colony PCR-based amplification with GoTaq Green (Promega, USA), RubyTaq (Affymetrix, USA), or Quick-Load Taq (New England Biolabs, USA) polymerase. Primers Rnd1-ARB1, Rnd1-ARB2, Rnd1-ARB3, and Rnd1-TnM20 were used for the first round of amplification. Primers Rnd2-ARB and Rnd2-TnM20 (Kulasekara *et al.*, 2005) were used for the second round of amplification.

Biofilm assays

Plates containing 40 ml of M6301 with 1% agar were poured fresh for each experiment and allowed to harden for 6–7 hours. *P. aeruginosa* cultures grown at 37°C for 6–8 h in 3 ml LB were back-diluted to an OD_{600} of 1.0, and 2 μl of the diluted cultures were spotted on

M6301 agar plates. The plates were incubated right-side-up at 25°C and were typically photographed after 4, 5, or 6 days, as indicated.

For further analysis, colonies were harvested from the agar surface and thoroughly resuspended by vortexing in 1 ml sterile PBS. Aliquots (100 μl) were removed from the resuspension to measure the optical density at 600 nm (OD_{600}) using a Genesys 20 spectrophotometer (Thermo Scientific, USA). The remaining volume was pelleted in a microcentrifuge at 13,000 *g* for 3 minutes at room temperature, and the supernatant was discarded. The pellets were resuspended in 1 ml of 40 μg/ml Congo red and were incubated with vigorous shaking on a vortex platform for at least 90 minutes at room temperature. The samples were again pelleted at 13,000 *g* for 3 minutes at room temperature, and the OD of the supernatants was measured at 490 nm. A standard curve was constructed by measuring the OD_{490} of Congo red at 40, 20, 10, 5, 2, 1, and 0.5 μg/ml. 1X PBS was used as a blank and as the diluent for the standard curve.

For *P. aeruginosa* biofilm assays conducted using a 96-well-plate format, stationary-phase LB liquid cultures grown for 6–8 h at 37°C were diluted 1:100 in M6301 or M6301R. The cultures were immediately plated in transparent Costar 96-well plates with lids (Fisher Scientific, USA) and were incubated at 25°C for 24 hours. The OD in each well was measured using a BioTek Synergy 2 plate reader (BioTek, USA) at 600 nm. The wells were then washed three times with dH_2O and stained with 0.1% crystal violet. After a 20-minute incubation at room temperature, the crystal violet was removed and the wells were again washed three times with dH_2O. After air-drying the plates overnight, the crystal violet was solubilized using 95% ethanol, and the OD_{600} was measured as described above. Biofilm biomass was calculated for each sample as the ratio of crystal violet staining to culture density.

Microscopy

Bacterial colonies were imaged with a Leica Wild M10 stereomicroscope with a Planapo 0.63X objective and a Diagnostic Instruments 18.2 Color Mosaic digital camera. Images were captured using Spot software v. 4.5 (Diagnostic Instruments).

Kinetic luciferase assay

Cultures of *P. aeruginosa* cells were grown in liquid LB shaking culture at 37°C to stationary phase and were then diluted to an OD_{600} of 1.0 in fresh LB. Aliquots (2 μl) of the resulting cultures were spotted on solid M6301, and plates were incubated at 25°C for 24, 72, or 120 hours. At the indicated time points, colonies were harvested in 1 ml sterile 1x PBS, homogenized for approximately 20 seconds, and plated in quadruplicate (200 μl each) in a 96-well polystyrene Costar plate (white with a clear bottom; Fisher Scientific, USA). Luciferase activity and OD were measured on a BioTek Synergy 2 plate reader (BioTek, USA). Luciferase luminescence was measured at a sensitivity setting of 200, and the culture OD was measured at 600 nm. In cases in which the culture OD exceeded the dynamic range of the reader, the analysis was repeated with two- or four-fold culture dilutions. Final luciferase activity values were calculated by normalizing luciferase luminescence to culture density.

Quantification of intracellular cyclic di-GMP

P. aeruginosa PA14 and derivative mutant strains were grown in 3 ml LB liquid shaking culture for 6–8 h at 37°C and spotted (2 μl each) at an OD_{600} of 1.0 on 40 ml M6301 agar as described above. After 4 d of growth at 25°C, the colonies were harvested for c-di-GMP extraction. We chose a 4-d time point after testing multiple incubation times, as it showed a clear distinction between our PA14 and Δ*amrZ* reference samples. Using a sterile spatula, the colonies were deposited into 5-ml Eppendorf™ tubes containing 1 ml sterile PBS and were homogenized for at least 20 seconds with an Argos pestle (Cole Parmer, USA). Cyclic di-GMP was extracted from triplicate biological samples and subjected to HPLC as previously described (Roy *et al.*, 2013). The quantity of c-di-GMP in each sample (calculated from a standard curve prepared from commercially available pure c-di-GMP) was normalized to the total amount of protein from the same sample (calculated using the Bradford method with bovine serum albumin standards).

Supplementary Material

Refer to Web version on PubMed Central for supplementary material.

Acknowledgments

We are grateful to Sunia Trauger for technical help with the HPLC experiments. We also thank members of the Losick lab for helpful discussions. M.T.C. was a Merck Postdoctoral Fellow of the Jane Coffin Childs Memorial Fund for Medical Research. S.A.L. was supported in part by the Natural Health Research Institute and the Tracie Lawlor Trust for Cystic Fibrosis. Funding was provided by the NIH (GM18568, to R.L.).

References

Ahuja EG, Janning P, Mentel M, Graebsch A, Breinbauer R, Hiller W, Costisella B, Thomashow LS, Mavrodi DV, Blankenfeldt W. PhzA/B catalyzes the formation of the tricycle in phenazine biosynthesis. J Am Chem Soc. 2008; 130:17053–17061. [PubMed: 19053436]

Alm RA, Hallinan JP, Watson AA, Mattick JS. Fimbrial biogenesis genes of *Pseudomonas aeruginosa*: *pilW* and *pilX* increase the similarity of type 4 fimbriae to the GSP protein-secretion systems and *pilY1* encodes a gonococcal PilC homologue. Mol Microbiol. 1996; 22:161–173. [PubMed: 8899718]

Boyd CD, O'Toole GA. Second messenger regulation of biofilm formation: breakthroughs in understanding c-di-GMP effector systems. Annu Rev Cell Dev Biol. 2012; 28:439–462. [PubMed: 23057745]

Branda SS, Chu F, Kearns DB, Losick R, Kolter R. A major protein component of the *Bacillus subtilis* biofilm matrix. Mol Microbiol. 2006; 59:1229–1238. [PubMed: 16430696]

Cabeen MT. Stationary phase-specific virulence factor overproduction by a *lasR* mutant of *Pseudomonas aeruginosa*. PLoS One. 2014; 9:e88743. [PubMed: 24533146]

Chu F, Kearns DB, Branda SS, Kolter R, Losick R. Targets of the master regulator of biofilm formation in *Bacillus subtilis*. Mol Microbiol. 2006; 59:1216–1228. [PubMed: 16430695]

Cotter PA, Stibitz S. c-di-GMP-mediated regulation of virulence and biofilm formation. Curr Opin Microbiol. 2007; 10:17–23. [PubMed: 17208514]

Dietrich LE, Okegbe C, Price-Whelan A, Sakhtah H, Hunter RC, Newman DK. Bacterial community morphogenesis is intimately linked to the intracellular redox state. J Bacteriol. 2013; 195:1371–1380. [PubMed: 23292774]

Drenkard E, Ausubel FM. *Pseudomonas* biofilm formation and antibiotic resistance are linked to phenotypic variation. Nature. 2002; 416:740–743. [PubMed: 11961556]

Driscoll JA, Brody SL, Kollef MH. The epidemiology, pathogenesis and treatment of *Pseudomonas aeruginosa* infections. Drugs. 2007; 67:351–368. [PubMed: 17335295]

Friedman L, Kolter R. Genes involved in matrix formation in *Pseudomonas aeruginosa* PA14 biofilms. Mol Microbiol. 2004a; 51:675–690. [PubMed: 14731271]

Friedman L, Kolter R. Two genetic loci produce distinct carbohydrate-rich structural components of the *Pseudomonas aeruginosa* biofilm matrix. J Bacteriol. 2004b; 186:4457–4465. [PubMed: 15231777]

Goodman AL, Kulasekara B, Rietsch A, Boyd D, Smith RS, Lory S. A signaling network reciprocally regulates genes associated with acute infection and chronic persistence in *Pseudomonas aeruginosa*. Dev Cell. 2004; 7:745–754. [PubMed: 15525535]

Haas D, Holloway BW, Schambock A, Leisinger T. The genetic organization of arginine biosynthesis in *Pseudomonas aeruginosa*. Mol Gen Genet. 1977; 154:7–22. [PubMed: 408599]

Hall-Stoodley L, Costerton JW, Stoodley P. Bacterial biofilms: from the natural environment to infectious diseases. Nat Rev Microbiol. 2004; 2:95–108. [PubMed: 15040259]

Heikaus CC, Pandit J, Klevit RE. Cyclic nucleotide binding GAF domains from phosphodiesterases: structural and mechanistic insights. Structure. 2009; 17:1551–1557. [PubMed: 20004158]

Hickman JW, Tifrea DF, Harwood CS. A chemosensory system that regulates biofilm formation through modulation of cyclic diguanylate levels. Proc Natl Acad Sci U S A. 2005; 102:14422–14427. [PubMed: 16186483]

Hobbs M, Collie ES, Free PD, Livingston SP, Mattick JS. PilS and PilR, a two-component transcriptional regulatory system controlling expression of type 4 fimbriae in *Pseudomonas aeruginosa*. Mol Microbiol. 1993; 7:669–682. [PubMed: 8097014]

Ishimoto KS, Lory S. Identification of *pilR*, which encodes a transcriptional activator of the *Pseudomonas aeruginosa* pilin gene. J Bacteriol. 1992; 174:3514–3521. [PubMed: 1317379]

Jones CJ, Newsom D, Kelly B, Irie Y, Jennings LK, Xu B, Limoli DH, Harrison JJ, Parsek MR, White P, Wozniak DJ. ChIP-Seq and RNA-Seq reveal an AmrZ-mediated mechanism for cyclic di-GMP synthesis and biofilm development by *Pseudomonas aeruginosa*. PLoS Pathog. 2014; 10:e1003984. [PubMed: 24603766]

Kearns DB, Chu F, Branda SS, Kolter R, Losick R. A master regulator for biofilm formation by *Bacillus subtilis*. Mol Microbiol. 2005; 55:739–749. [PubMed: 15661000]

Kim HJ, Lee CR, Kim M, Peterkofsky A, Seok YJ. Dephosphorylated NPr of the nitrogen PTS regulates lipid A biosynthesis by direct interaction with LpxD. Biochem Biophys Res Commun. 2011; 409:556–561. [PubMed: 21605551]

Kuchma SL, Brothers KM, Merritt JH, Liberati NT, Ausubel FM, O'Toole GA. BifA, a cyclic-Di-GMP phosphodiesterase, inversely regulates biofilm formation and swarming motility by *Pseudomonas aeruginosa* PA14. J Bacteriol. 2007; 189:8165–8178. [PubMed: 17586641]

Kulasakara H, Lee V, Brencic A, Liberati N, Urbach J, Miyata S, Lee DG, Neely AN, Hyodo M, Hayakawa Y, Ausubel FM, Lory S. Analysis of *Pseudomonas aeruginosa* diguanylate cyclases and phosphodiesterases reveals a role for bis-(3′–5′)-cyclic-GMP in virulence. Proc Natl Acad Sci U S A. 2006; 103:2839–2844. [PubMed: 16477007]

Kulasekara HD, Ventre I, Kulasekara BR, Lazdunski A, Filloux A, Lory S. A novel two-component system controls the expression of *Pseudomonas aeruginosa* fimbrial cup genes. Mol Microbiol. 2005; 55:368–380. [PubMed: 15659157]

Lee CR, Cho SH, Yoon MJ, Peterkofsky A, Seok YJ. *Escherichia coli* enzyme IIANtr regulates the K+ transporter TrkA. Proc Natl Acad Sci U S A. 2007a; 104:4124–4129. [PubMed: 17289841]

Lee CR, Park YH, Kim M, Kim YR, Park S, Peterkofsky A, Seok YJ. Reciprocal regulation of the autophosphorylation of enzyme INtr by glutamine and alpha-ketoglutarate in *Escherichia coli*. Mol Microbiol. 2013; 88:473–485. [PubMed: 23517463]

Lee VT, Matewish JM, Kessler JL, Hyodo M, Hayakawa Y, Lory S. A cyclic-di-GMP receptor required for bacterial exopolysaccharide production. Mol Microbiol. 2007b; 65:1474–1484. [PubMed: 17824927]

Lepine F, Milot S, Deziel E, He J, Rahme LG. Electrospray/mass spectrometric identification and analysis of 4-hydroxy-2-alkylquinolines (HAQs) produced by *Pseudomonas aeruginosa*. J Am Soc Mass Spectrom. 2004; 15:862–869. [PubMed: 15144975]

Longo F, Rampioni G, Bondi R, Imperi F, Fimia GM, Visca P, Zennaro E, Leoni L. A new transcriptional repressor of the *Pseudomonas aeruginosa* quorum sensing receptor gene *lasR*. PLoS One. 2013; 8:e69554. [PubMed: 23861975]

Lüttmann D, Heermann R, Zimmer B, Hillmann A, Rampp IS, Jung K, Görke B. Stimulation of the potassium sensor KdpD kinase activity by interaction with the phosphotransferase protein IIA(Ntr) in *Escherichia coli*. Mol Microbiol. 2009; 72:978–994. [PubMed: 19400808]

McLoon AL, Guttenplan SB, Kearns DB, Kolter R, Losick R. Tracing the Domestication of a Biofilm-Forming Bacterium. J Bacteriol. 2011

Merritt JH, Brothers KM, Kuchma SL, O'Toole GA. SadC reciprocally influences biofilm formation and swarming motility via modulation of exopolysaccharide production and flagellar function. J Bacteriol. 2007; 189:8154–8164. [PubMed: 17586642]

Merritt JH, Ha DG, Cowles KN, Lu W, Morales DK, Rabinowitz J, Gitai Z, O'Toole GA. Specific control of *Pseudomonas aeruginosa* surface-associated behaviors by two c-di-GMP diguanylate cyclases. MBio. 2010; 1

Nguyen D, Joshi-Datar A, Lepine F, Bauerle E, Olakanmi O, Beer K, McKay G, Siehnel R, Schafhauser J, Wang Y, Britigan BE, Singh PK. Active starvation responses mediate antibiotic tolerance in biofilms and nutrient-limited bacteria. Science. 2011; 334:982–986. [PubMed: 22096200]

O'Toole GA, Kolter R. Flagellar and twitching motility are necessary for *Pseudomonas aeruginosa* biofilm development. Mol Microbiol. 1998a; 30:295–304. [PubMed: 9791175]

O'Toole GA, Kolter R. Initiation of biofilm formation in *Pseudomonas fluorescens* WCS365 proceeds via multiple, convergent signalling pathways: a genetic analysis. Mol Microbiol. 1998b; 28:449–461. [PubMed: 9632250]

Parkins MD, Ceri H, Storey DG. *Pseudomonas aeruginosa* GacA, a factor in multihost virulence, is also essential for biofilm formation. Mol Microbiol. 2001; 40:1215–1226. [PubMed: 11401724]

Pfluger-Grau K, Gorke B. Regulatory roles of the bacterial nitrogen-related phosphotransferase system. Trends Microbiol. 2010; 18:205–214. [PubMed: 20202847]

Powell BS, Court DL, Inada T, Nakamura Y, Michotey V, Cui X, Reizer A, Saier MH Jr, Reizer J. Novel proteins of the phosphotransferase system encoded within the *rpoN* operon of *Escherichia coli*. Enzyme IIANtr affects growth on organic nitrogen and the conditional lethality of an erats mutant. J Biol Chem. 1995; 270:4822–4839. [PubMed: 7876255]

Rabus R, Reizer J, Paulsen I, Saier MH Jr. Enzyme I(Ntr) from *Escherichia coli*. A novel enzyme of the phosphoenolpyruvate-dependent phosphotransferase system exhibiting strict specificity for its phosphoryl acceptor, NPr. J Biol Chem. 1999; 274:26185–26191. [PubMed: 10473571]

Richards MJ, Edwards JR, Culver DH, Gaynes RP. Nosocomial infections in combined medical-surgical intensive care units in the United States. Infect Control Hosp Epidemiol. 2000; 21:510–515. [PubMed: 10968716]

Roy AB, Petrova OE, Sauer K. Extraction and Quantification of Cyclic Di-GMP from. Bio Protoc. 2013; 3

Semmler AB, Whitchurch CB, Leech AJ, Mattick JS. Identification of a novel gene, *fimV*, involved in twitching motility in *Pseudomonas aeruginosa*. Microbiology. 2000; 146(Pt 6):1321–1332. [PubMed: 10846211]

Starkey M, Hickman JH, Ma L, Zhang N, Long SDe, Hinz A, Palacios S, Manoil C, Kirisits MJ, Starner TD, Wozniak DJ, Harwood CS, Parsek MR. *Pseudomonas aeruginosa* rugose small-colony variants have adaptations that likely promote persistence in the cystic fibrosis lung. J Bacteriol. 2009; 191:3492–3503. [PubMed: 19329647]

Vallet I, Olson JW, Lory S, Lazdunski A, Filloux A. The chaperone/usher pathways of *Pseudomonas aeruginosa*: identification of fimbrial gene clusters (*cup*) and their involvement in biofilm formation. Proc Natl Acad Sci U S A. 2001; 98:6911–6916. [PubMed: 11381121]

van Montfort RL, Dijkstra BW. The functional importance of structural differences between the mannitol-specific IIAmannitol and the regulatory IIAnitrogen. Protein Sci. 1998; 7:2210–2216. [PubMed: 9792109]

Ventre I, Goodman AL, Vallet-Gely I, Vasseur P, Soscia C, Molin S, Bleves S, Lazdunski A, Lory S, Filloux A. Multiple sensors control reciprocal expression of *Pseudomonas aeruginosa* regulatory RNA and virulence genes. Proc Natl Acad Sci U S A. 2006; 103:171–176. [PubMed: 16373506]

Wang C, Ye F, Kumar V, Gao YG, Zhang LH. BswR controls bacterial motility and biofilm formation in *Pseudomonas aeruginosa* through modulation of the small RNA rsmZ. Nucleic Acids Res. 2014; 42:4563–4576. [PubMed: 24497189]

Wehbi H, Portillo E, Harvey H, Shimkoff AE, Scheurwater EM, Howell PL, Burrows LL. The peptidoglycan-binding protein FimV promotes assembly of the *Pseudomonas aeruginosa* type IV pilus secretin. J Bacteriol. 2011; 193:540–550. [PubMed: 21097635]

Yoon SS, Karabulut AC, Lipscomb JD, Hennigan RF, Lymar SV, Groce SL, Herr AB, Howell ML, Kiley PJ, Schurr MJ, Gaston B, Choi KH, Schweizer HP, Hassett DJ. Two-pronged survival strategy for the major cystic fibrosis pathogen, *Pseudomonas aeruginosa*, lacking the capacity to degrade nitric oxide during anaerobic respiration. EMBO J. 2007; 26:3662–3672. [PubMed: 17627281]

Zimmer B, Hillmann A, Gorke B. Requirements for the phosphorylation of the *Escherichia coli* EIIANtr protein in vivo. FEMS Microbiol Lett. 2008; 286:96–102. [PubMed: 18625021]

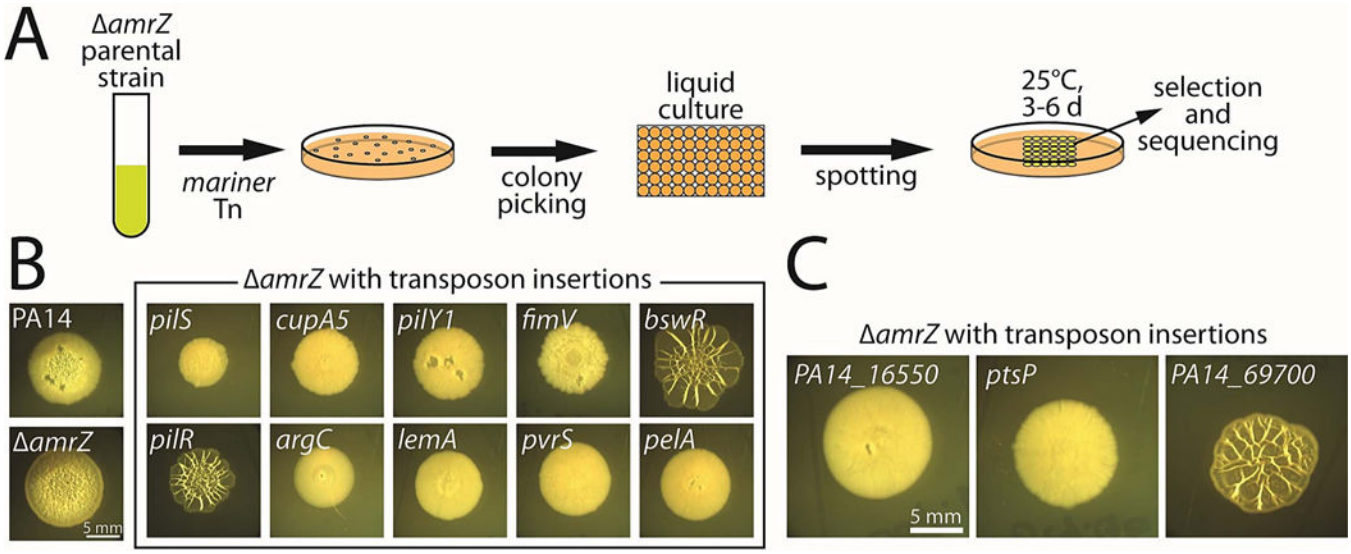

Figure 1. A visual colony-morphology screen for biofilm-related genes in *P. aeruginosa*

A. Schematic of the colony-morphology screen. The *amrZ*-deleted parental strain was mutagenized with a *Mariner*-based transposon, and individual mutant colonies were then grown overnight in static liquid culture before being spotted in an array on M6301-1% agar plates and grown at 25°C for 4–6 days. Visual inspection of the colonies was used to select promising candidates for subsequent sequencing to identify the position of transposon insertion. B. Colony morphologies (4 d) of mutants identified in the screen with known roles in biofilm formation. C. Colony morphologies (4 d) of mutants identified in the screen with no previously described role in biofilm formation.

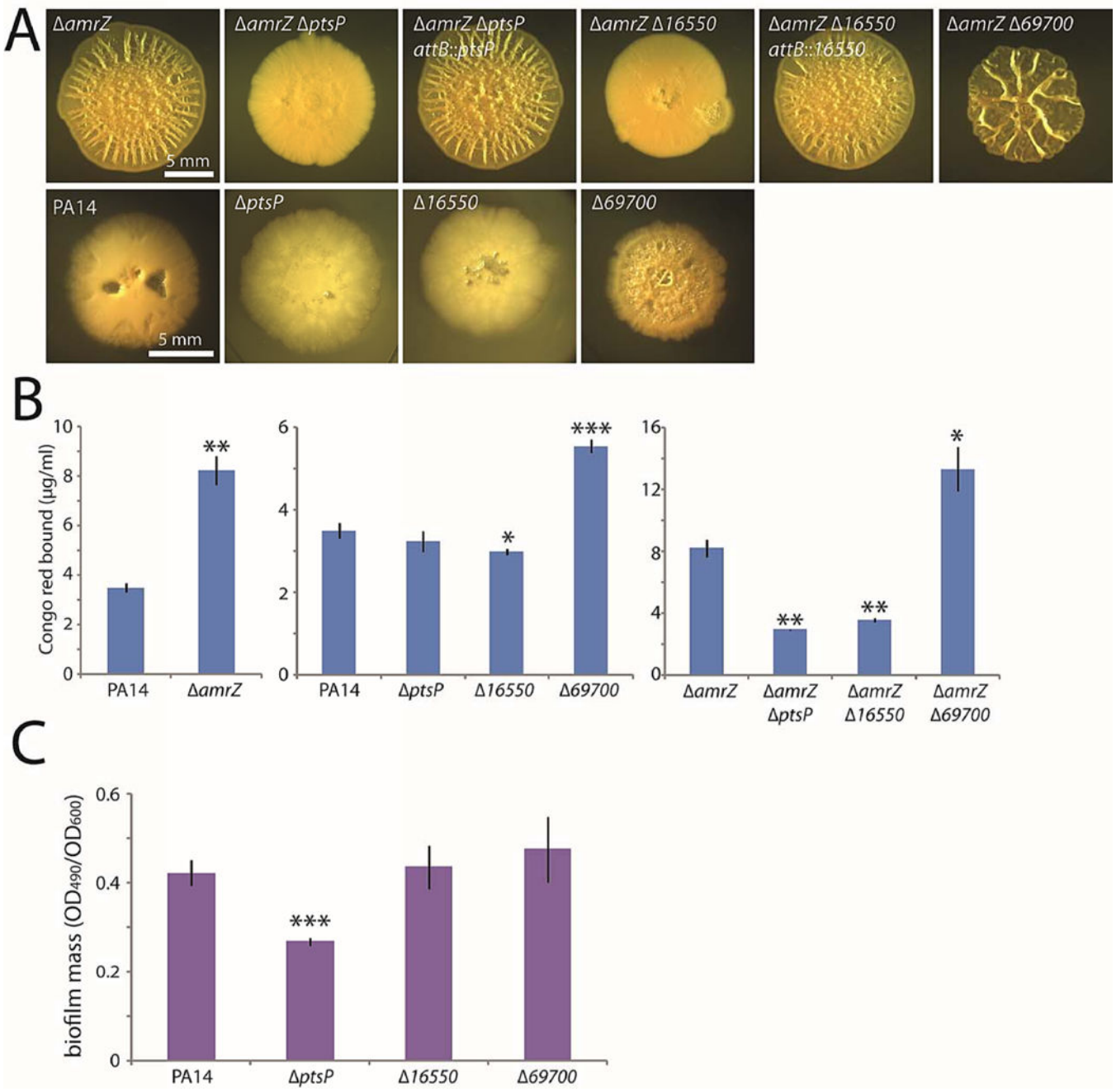

Figure 2. Three genes with previously unknown roles in biofilm formation

A. Colony morphologies (4–5 d) of strains bearing markerless in-frame deletions of the three new genes identified in the screen. In the *amrZ* deletion background, deletions were complemented at the ectopic *attB* locus. B. Congo red binding by the indicated mutant colonies. Mean values of at least 3 replicates are shown; error bars indicate ± 1 standard deviation. *, $p < 0.05$; **, $p < 0.01$; ***, $p < 0.001$ relative to the leftmost strain in each graph. C. Crystal violet binding by the indicated mutants after 24 h of static culture. Mean values of at least 4 replicates are shown; error bars indicate ± 1 standard deviation. ***, $p < 0.001$ relative to PA14.

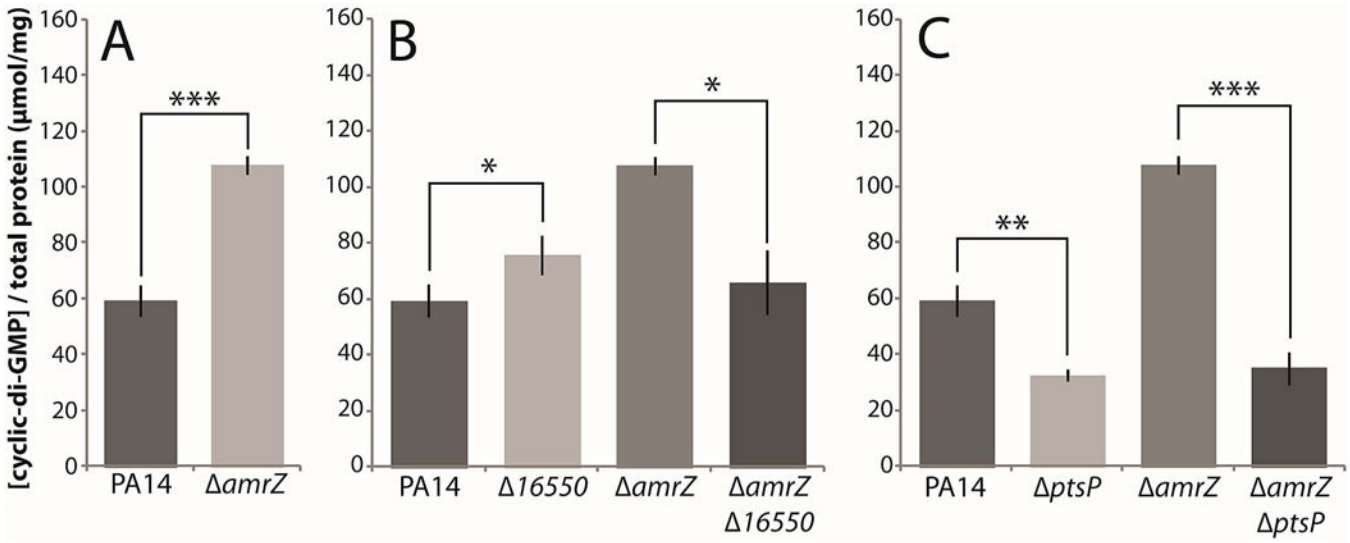

Figure 3. Deletions of *16550* and *ptsP* reduce cellular c-di-GMP levels

Cellular c-di-GMP was extracted from homogenized colonies and measured by HPLC. A. c-di-GMP levels in the parental PA14 and *amrZ* deletion strains. B. c-di-GMP levels in *16550* mutants. C. c-di-GMP levels in *ptsP* mutants. Mean values of at least 3 replicates are shown; error bars indicate ± 1 standard deviation. *, $p < 0.05$; **, $p < 0.01$; ***, $p < 0.001$.

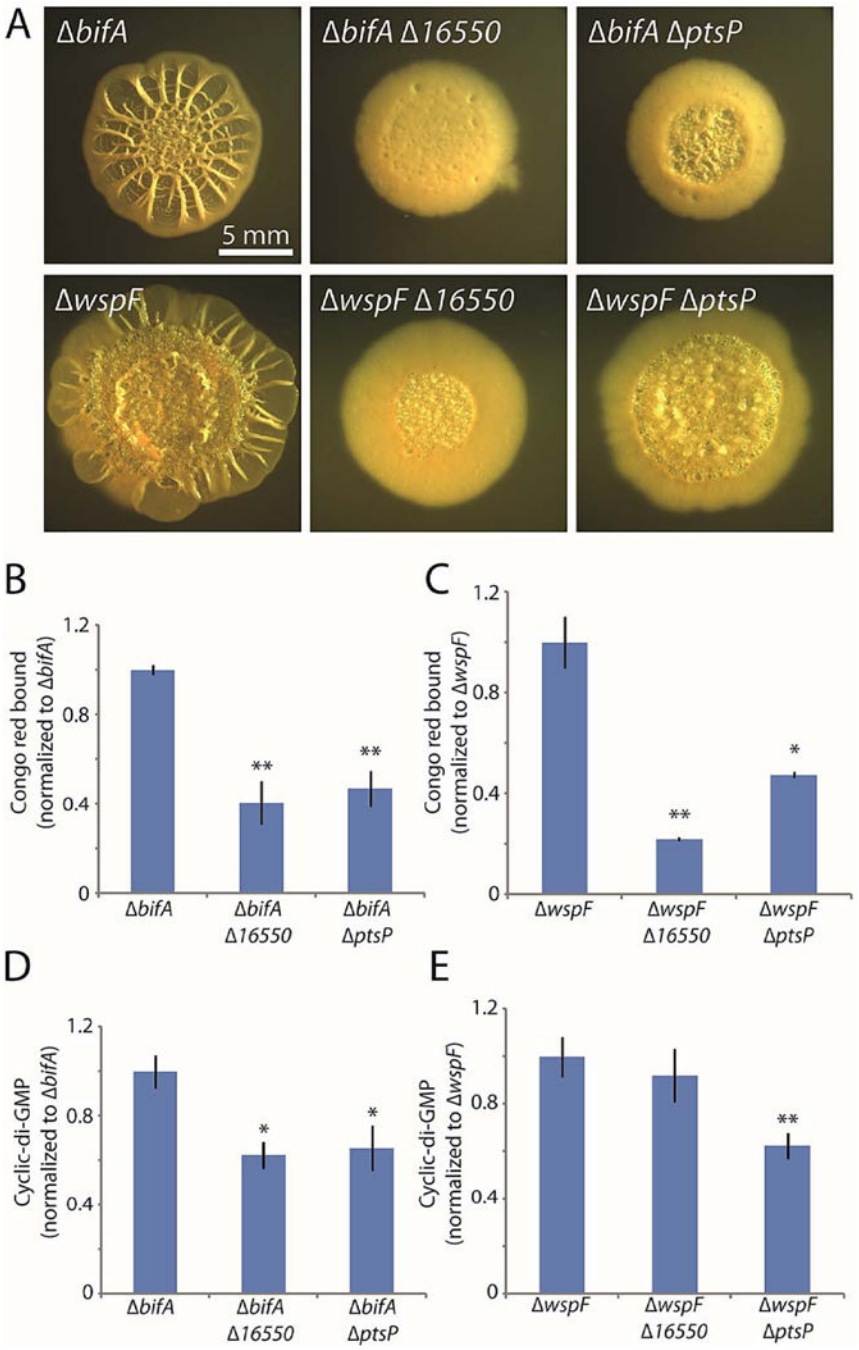

Figure 4. Deletions of *16550* and *ptsP* reduce biofilm formation by *bifA* and *wspF* mutants

A. Colony morphologies (4 d for *bifA*, 6 d for *wspF*) of strains bearing markerless *bifA* or *wspF* deletions alone or in combination with markerless in-frame deletions of the three new genes identified in the screen. B and C. Congo red binding by the indicated colonies. D and E. c-di-GMP levels in the indicated colonies. For panels B–E, the mean values of at least 3 replicates are shown; error bars indicate ± 1 standard deviation. *, $p < 0.05$; **, $p < 0.01$ relative to the single mutants shown at the left of each graph.

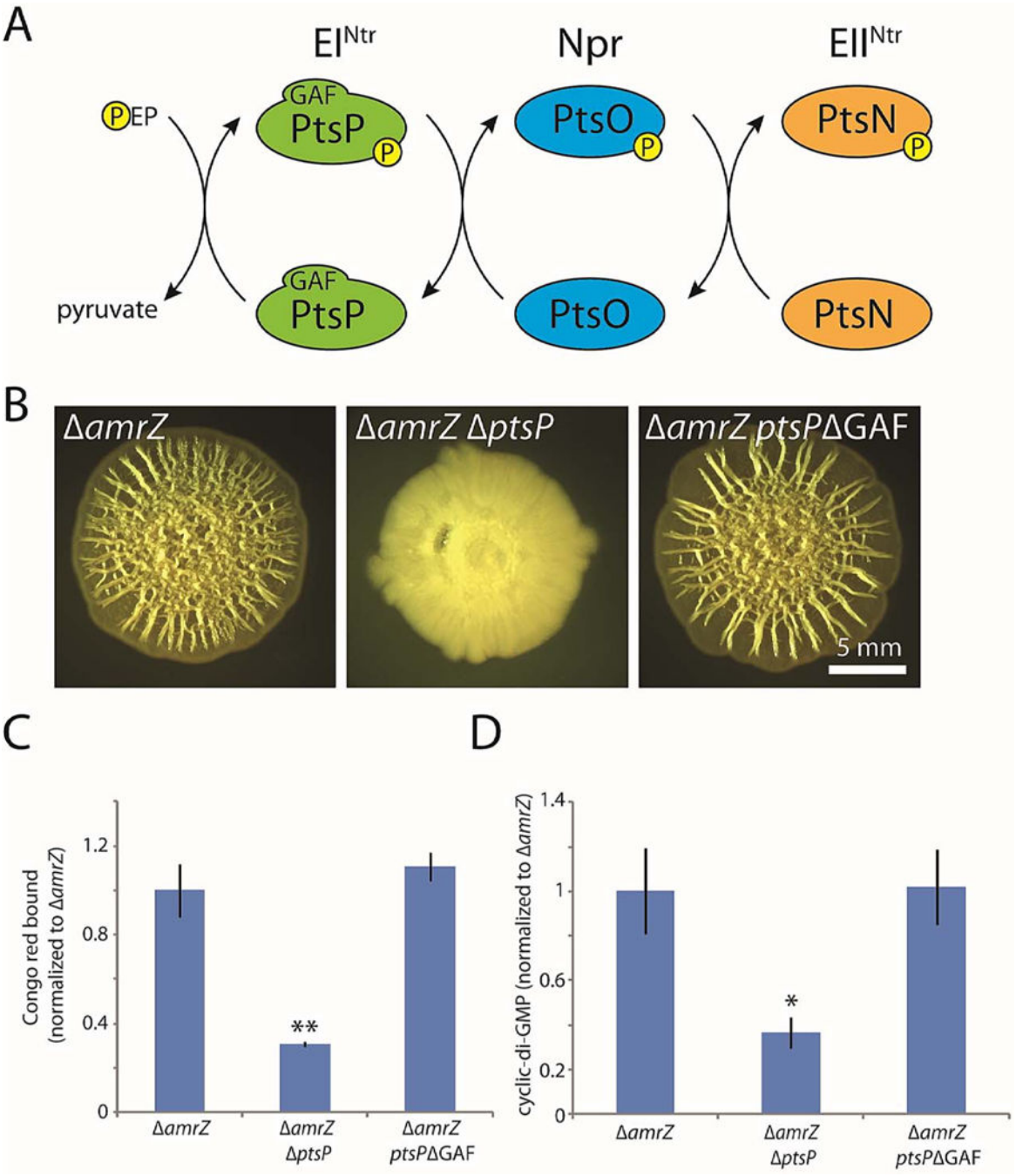

Figure 5. The GAF domain of PtsP is dispensable for its role in biofilm formation

A. Schematic of the PTS^{Ntr} phosphorylation cascade. Phosphate is transferred by EI^{Ntr} (encoded by *ptsP*) from phosphoenolpyruvate (PEP) to Npr (encoded by *ptsO*). Npr in turn transfers the phosphate to EII^{Ntr} (encoded by *ptsN*), which is thought to directly exert regulatory activity. B. Colony morphologies (6 d) of the indicated strains, including a strain in which the native copy of *ptsP* has been markerlessly replaced with a copy deleted for nucleotides 49–492, which encode the 148-residue GAF domain of EI^{Ntr}. C. Congo red binding by the indicated colonies. Mean values of at least 3 replicates are shown; error bars

indicate ± 1 standard deviation. **, $p < 0.01$ relative to *amrZ*. D. c-di-GMP levels in the indicated colonies. Mean values of at least 3 replicates are shown; error bars indicate ± 1 standard deviation. *, $p < 0.05$ relative to *amrZ*.

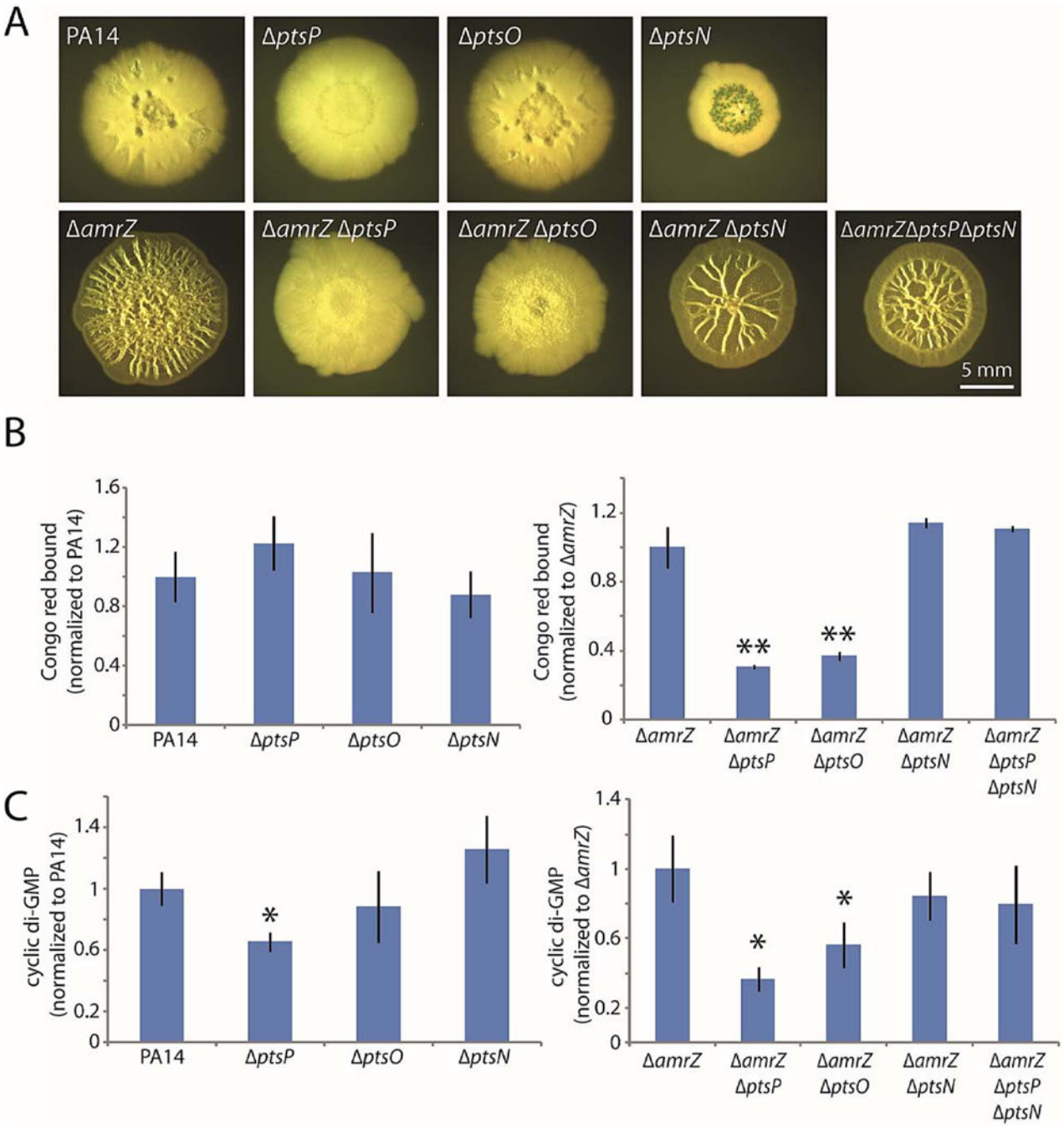

Figure 6. Unphosphorylated EII^{Ntr} (PtsN) is responsible for the biofilm-suppressing effect of PTS^{Ntr} mutants

A. Colony morphologies (6 d) of the indicated strains with combinations of PTS^{Ntr} deletions. B. Congo red binding by the indicated colonies. Mean values of at least 3 replicates are shown; error bars indicate ± 1 standard deviation. **, $p < 0.01$ relative to *amrZ*. C. c-di-GMP levels in the indicated colonies. Mean values of at least 3 replicates are shown; error bars indicate ± 1 standard deviation. *, $p < 0.05$ relative to *amrZ*.

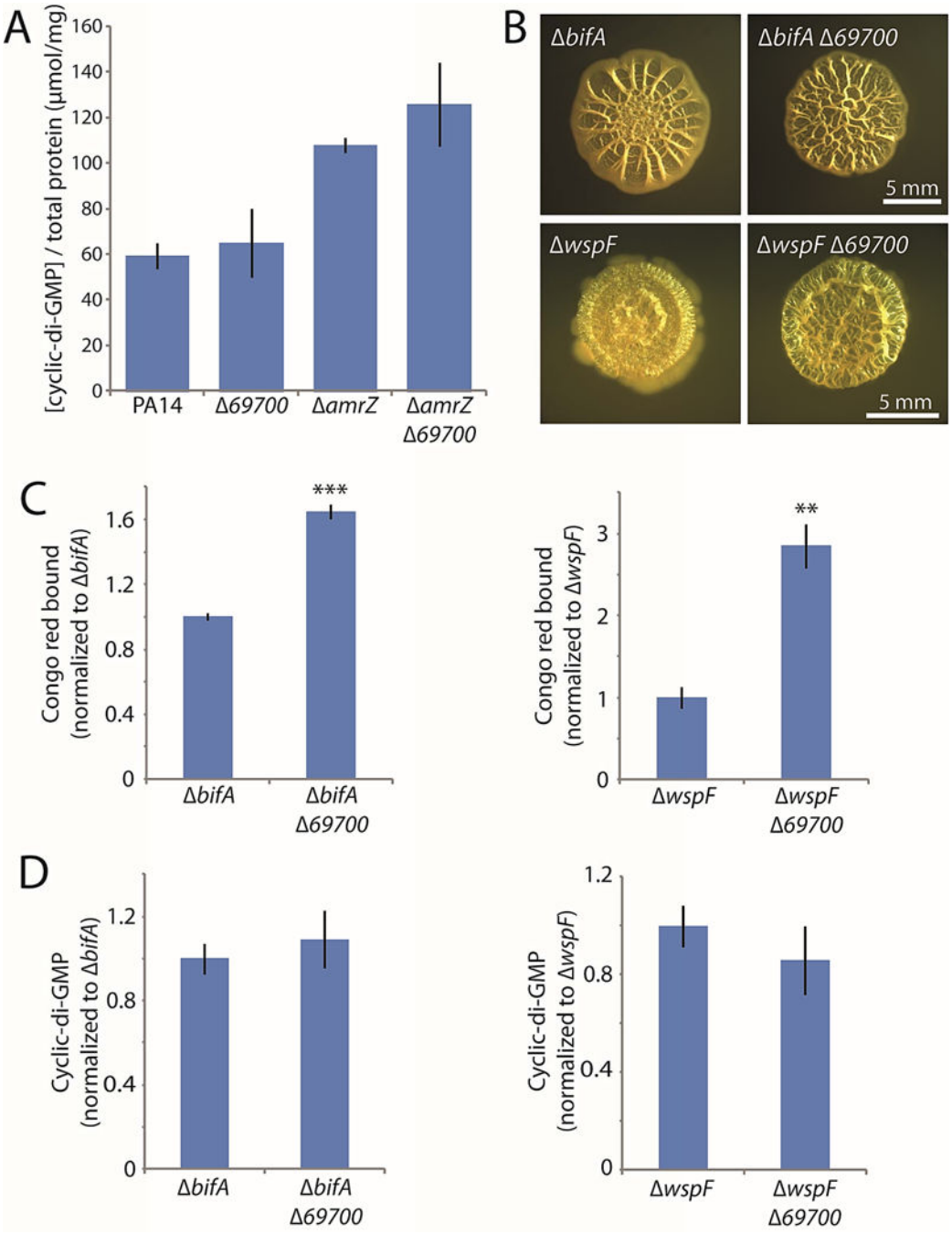

Figure 7. Deletion of *69700* increases biofilm formation but not cellular c-di-GMP

A. c-di-GMP levels in the indicated *69700* mutants. B. Colony morphologies (4 d) of strains bearing markerless *bifA* or *wspF* deletions alone or in combination with *69700* deletions. C. Congo red binding by the indicated colonies. D. c-di-GMP levels in the indicated colonies. For panels C and D, the mean values of at least 3 replicates are shown; error bars indicate ± 1 standard deviation. **, $p < 0.01$; ***, $p < 0.001$ relative to the single mutants shown at the left of each graph.

Table 1

Pseudomonas aeruginosa strains used in this study.

Strain	Genotype or description	Source or reference
PA14 (MTC1)	Laboratory wild-type strain of *P. aeruginosa*	Laboratory stock; Stephen Lory, Harvard Medical School
MTC590	PA14 Δ*amrZ*	This study
MTC1240	PA14 Δ*amrZ* Tn*69700* isolate 1, $Gent^R$	This study
MTC1241	PA14 Δ*amrZ* Tn*16550*, $Gent^R$	This study
MTC1281	PA14 Δ*amrZ* Tn*ptsP*, $Gent^R$	This study
MTC1284	PA14 Δ*amrZ* Tn*69700* isolate 2, $Gent^R$	This study
MTC1381	PA14 Δ*amrZ* Δ*16550*	This study
MTC1387	PA14 Δ*amrZ* Δ*ptsP*	This study
MTC1398	PA14 Δ*amrZ* Δ*69700*	This study
MTC1448	PA14 Δ*16550*	This study
MTC1450	PA14 Δ*ptsP*	This study
MTC1512	PA14 Δ*69700*	This study
MTC1521	PA14 Δ*bifA*	This study
MTC1522	PA14 Δ*bifA* Δ*16550*	This study
MTC1523	PA14 Δ*bifA* Δ*69700*	This study
MTC1525	PA14 Δ*bifA* Δ*ptsP*	This study
MTC1533	PA14 *attB*::CTX-1-P_{adcA} -lux, Tet^R	This study
MTC1535	PA14 Δ*amrZ attB*::CTX-1-P_{adcA} -lux	This study
MTC1537	PA14 Δ*amrZ* Δ*16550 attB*::CTX-1-P_{adcA} -lux, Tet^R	This study
MTC1539	PA14 Δ*amrZ* Δ*69700 attB*::CTX-1-P_{adcA} -lux, Tet^R	This study
MTC1541	PA14 Δ*amrZ* Δ*ptsP attB*::CTX-1-P_{adcA} -lux, Tet^R	This study
MTC1543	PA14 Δ*amrZ* Δ*ptsP* CTX-1-*ptsP*, Tet^R	This study
MTC1549	PA14 Δ*amrZ* Δ*16550* CTX-1-*16550*, Tet^R	This study
MTC1562	PA14 Δ*amrZ* Δ*adcA*	This study
MTC1603	PA14 Δ*amrZ* Δ*ptsO*	This study
MTC1605	PA14 Δ*amrZ* $ptsP_{\Delta GAF}$	This study
MTC1649	PA14 Δ*ptsN*	This study
MTC1651	PA14 Δ*amrZ* Δ*ptsN*	This study
MTC1666	PA14 Δ*amrZ* Δ*ptsN* Δ*ptsP*	This study
MTC1709	PA14 Δ*wspF*	This study
MTC1711	PA14 Δ*wspF* Δ*ptsP*	This study
MTC1713	PA14 Δ*ptsO*	This study
MTC1714	PA14 Δ*wspF* Δ*16550*	This study
MTC1717	PA14 Δ*wspF* Δ*69700*	This study